




Discrete spectrum radiation from a charged particle moving in a medium with Maxwell's fish-eye refraction-index profile

Zhyrair Gevorkian ^{1,2,*} and Mher Davtyan ²

¹*Yerevan Physics Institute, Alikhanian Brothers St. 2, 0036, Yerevan, Armenia*

²*Institute of Radiophysics and Electronics, Ashtarak-2, 0203, Armenia*

 (Received 11 June 2020; accepted 10 November 2020; published 3 December 2020)

Radiation from a charged particle moving in a medium with a Maxwell's fish-eye refraction index profile is considered. It is shown that the radiation spectrum has a discrete character. The main emitted wavelength is proportional to the refractive profile's radius and has a dipole character in a regular medium. A Cherenkov-like threshold velocity is established. A cardinal rearrangement of angular distribution in a lossless medium is predicted. This behavior is caused by the total internal reflection in a lossless medium as opposed to photons' attenuated total reflection in the regular medium. A lossless medium ensures that both directed and monochromatic emission can serve as a light source in the corresponding regions.

DOI: [10.1103/PhysRevA.102.063504](https://doi.org/10.1103/PhysRevA.102.063504)

I. INTRODUCTION

Recently the interest in the Maxwell's fish-eye [1] refraction index profile has increased dramatically. The reasons are its possible use in cloaking phenomena [2], perfect imaging [3–6], quantum optics with single atoms and photons [7], optical resonators [8,9], etc. Earlier we showed [9] that apart from the spherical symmetry, Maxwell's fish eye possesses an additional symmetry. The extended symmetry leads to additional integrals of motion. In the geometrical optics limit, all the photon trajectories are closed and their parameters are expressed through the integrals of motion [9]. To detect a cloak in Maxwell's fish-eye medium, it was suggested [10] to use the radiation induced by the motion of a charged particle. Consideration was realized by exploring the dyadic Green's functions [11]. It was revealed that the emitted radiation is a mix of Cherenkov and transition radiations.

As apposed to the research regarding light propagation in Maxwell's fish-eye medium, much less attention has been paid to light generation problems in that particular medium. However, it turns out that radiation emitted by a charged particle when it passes through such a medium possesses unique properties as well (see below). In the present paper, we consider the spectrum and angular distribution of radiation from a charged particle moving in Maxwell's fish-eye refraction profile medium. Instead of dyadic Green's function, we utilize the exact Green's function of the scalar Helmholtz equation [12–14]. This approach allows us to obtain complete analytical expressions for radiation intensity that reveal physical results.

II. INITIAL RELATIONS

We start from Maxwell's equations for the field Fourier components:

$$\nabla \times \mathbf{E}(\mathbf{r}, \omega) = \frac{i\omega}{c} \mathbf{B}(\mathbf{r}, \omega),$$

$$\begin{aligned} \nabla \times \mathbf{H}(\mathbf{r}, \omega) &= \frac{4\pi}{c} \mathbf{j}(\mathbf{r}, \omega) - \frac{i\omega}{c} \mathbf{D}(\mathbf{r}, \omega), \\ \nabla \cdot \mathbf{D} &= 4\pi \rho(\mathbf{r}, \omega), \quad \nabla \cdot \mathbf{B} = 0, \\ \mathbf{B}(\mathbf{r}, \omega) &= \mu(\mathbf{r}, \omega) \mathbf{H}(\mathbf{r}, \omega), \\ \mathbf{D}(\mathbf{r}, \omega) &= \varepsilon(\mathbf{r}, \omega) \mathbf{E}(\mathbf{r}, \omega). \end{aligned} \quad (1)$$

where ρ and \mathbf{j} are the charge and current densities associated with the moving particle. We proceed with the calculations using vector potential \mathbf{A} and scalar potential ϕ instead of \mathbf{E} and \mathbf{B} . From Eq. (1) those can be introduced in the following way:

$$\mathbf{B} = \nabla \times \mathbf{A}, \quad \mathbf{E} - \frac{i\omega}{c} \mathbf{A} = \nabla \phi. \quad (2)$$

By substituting the expressions for E and B into the second equation in Eq. (1), we get to the following equation:

$$\nabla \times \frac{1}{\mu} \nabla \times \mathbf{A} = \frac{4\pi}{c} \mathbf{j} - \frac{i\omega}{c} \varepsilon (\nabla \phi + \frac{i\omega}{c} \mathbf{A}). \quad (3)$$

From Eq. (3), assuming that $\mu(\mathbf{r}, \omega)$ is a slowly varying function in the space and using the property of a double curl, we obtain

$$\begin{aligned} \nabla^2 \mathbf{A} + \frac{\omega^2}{c^2} \varepsilon(\mathbf{r}) \mu(\mathbf{r}) \mathbf{A} \\ = -\frac{4\pi}{c} \mu \mathbf{j} + \nabla (\nabla \cdot \mathbf{A}) + \frac{i\omega}{c} \varepsilon(\mathbf{r}) \mu(\mathbf{r}) \nabla \phi. \end{aligned} \quad (4)$$

We take the gauge condition for an inhomogeneous medium in the following form:

$$\nabla (\nabla \cdot \mathbf{A}) + \frac{i\omega}{c} \varepsilon(\mathbf{r}) \mu(\mathbf{r}) \nabla \phi = 0 \quad (5)$$

and eventually find the equation for the vector potential

$$\nabla^2 \mathbf{A} + \frac{\omega^2}{c^2} \varepsilon(\mathbf{r}) \mu(\mathbf{r}) \mathbf{A} = -\frac{4\pi}{c} \mu \mathbf{j}. \quad (6)$$

*Corresponding author: gevork@yerphi.am

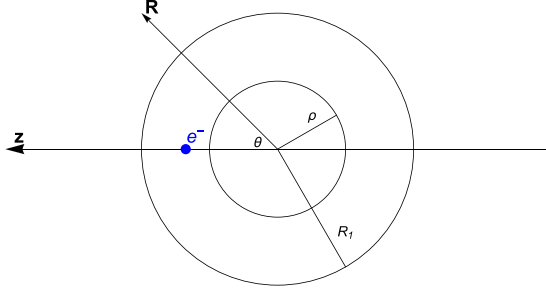


FIG. 1. Geometry of the problem. Observation point is far from the charge and from the core of the refraction profile.

Note that although the condition (5) is similar to the Lorenz gauge condition for inhomogeneous media, it does not result in completely decoupled equations for vector and scalar potentials. However, our choice of the gauge condition leads to a less complex equation for the vector potential, which is more important when examining problems regarding radiation. Note also that when deriving Eq. (6) we assume the slow variance only for $\mu(\mathbf{r})$ but not for $\varepsilon(\mathbf{r})$. This means that our consideration is correct for quite a large class of materials (particularly all nonmagnetic mediums $\mu = 1$). Also note that the form of the equation for \mathbf{A} can be changed depending on the gauge condition we choose [15]. The point is that in an inhomogeneous medium the Lorenz gauge condition acquires different forms [15]. Again here we choose the one that leads to the simplest equation for the vector potential.

$$G_\nu(\mathbf{R}, \mathbf{r}) = -\frac{1}{4\pi \cos(\pi\nu)} \frac{\sqrt{(R^2 + \rho^2)(r^2 + \rho^2)}}{|\mathbf{R} - \mathbf{r}| \sqrt{R^2 r^2 + 2\rho^2 \mathbf{R}\mathbf{r} + \rho^4}} \sin \left\{ (v + 1/2) \arccos \left[-1 + \frac{2\rho^2(\mathbf{R} - \mathbf{r})^2}{(R^2 + \rho^2)(r^2 + \rho^2)} \right] \right\}, \quad (10)$$

where

$$v = \frac{-1 + \sqrt{1 + 4n_0^2 k^2 \rho^2}}{2}. \quad (11)$$

Here $k = \omega/c$ and $v \neq m + 1/2, -m - 3/2$ ($m \in \mathbb{N}$). At these specific values, as it is seen from Eq. (10), Green's function is divergent and one needs another expression [13]:

$$\begin{aligned} \tilde{G}_{m+1/2}(\mathbf{R}, \mathbf{r}) = & (-)^m \frac{1}{4\pi^2} \frac{\sqrt{(R^2 + \rho^2)(r^2 + \rho^2)}}{|\mathbf{R} - \mathbf{r}| \sqrt{R^2 r^2 + 2\rho^2 \mathbf{R}\mathbf{r} + \rho^4}} \left(\cos \left\{ (m + 1) \arccos \left[-1 + \frac{2\rho^2(\mathbf{R} - \mathbf{r})^2}{(R^2 + \rho^2)(r^2 + \rho^2)} \right] \right\} \right. \\ & \left. \times \arccos \left[-1 + \frac{2\rho^2(\mathbf{R} - \mathbf{r})^2}{(R^2 + \rho^2)(r^2 + \rho^2)} \right] + \frac{\sin \left\{ (m + 1) \arccos \left[-1 + \frac{2\rho^2(\mathbf{R} - \mathbf{r})^2}{(R^2 + \rho^2)(r^2 + \rho^2)} \right] \right\}}{2(m + 1)} \right). \quad (12) \end{aligned}$$

The current density corresponding to the particle with charge e moving along the z axis with velocity v has the form $\mathbf{j}(\mathbf{r}, t) = ev\delta(x)\delta(y)\delta(z - vt)$. The corresponding Fourier component which determines the Fourier component of the radiation vector potential will have the following form:

$$\mathbf{j}(\mathbf{r}, \omega) = \frac{e\mathbf{v}}{v} \delta(x)\delta(y)e^{ik_0 z}, \quad (13)$$

where $k_0 = \omega/v$. Using the expressions for Green's functions Eqs. (10) and (12) and the expression for the current density (13), one can find radiation potential and radiation intensity.

It follows from Eq. (6) that the radiation vector potential associated with the external source is directed similarly to current density \mathbf{j} , which is assumed to be directed along z ; see Fig. 1. Therefore the radiation potential can be expressed through Green's function of the scalar Helmholtz equation

$$A_{zr}(\mathbf{R}) = -\frac{4\pi}{c} \int d\mathbf{r} G(\mathbf{R}, \mathbf{r}) \mu(\mathbf{r}) j_z(\mathbf{r}). \quad (7)$$

This equation represents a particular solution of Eq. (6) associated with an external source. To obtain the general solution, one should add also the solution of a homogeneous equation. However, when examining the far-field radiation, it is the particular solution (7) that gives the main contribution. Green's function satisfies the equation

$$\left[\nabla^2 + \frac{\omega^2}{c^2} n^2(\mathbf{R}) \right] G(\mathbf{R}, \mathbf{r}) = \delta(\mathbf{R} - \mathbf{r}), \quad (8)$$

where $n(\mathbf{r}) = \sqrt{\varepsilon(\mathbf{r})\mu(\mathbf{r})}$ is the refraction index of the medium. We choose it in the form (see Fig. 1)

$$n(r) = \begin{cases} \frac{2n_0\rho^2}{r^2 + \rho^2}, & r < R_1 \\ 1, & r > R_1. \end{cases} \quad (9)$$

Green's problem (8) is exactly solved [12,13]:

III. RADIATION POTENTIAL

First, we determine the radiation potential in the region $R < R_1$:

$$A(\mathbf{R}) = -\frac{4\pi}{c} \int_{r < R_1} d\mathbf{r} G(\mathbf{R}, \mathbf{r}) \mu(\mathbf{r}) j(\mathbf{r}), \quad R < R_1. \quad (14)$$

Here $A \equiv A_z, j \equiv j_z$. According to Green's theorem, in Eq. (14) should also appear an additional surface integral over the sphere of radius R_1 . However, for large $R_1 \gg \rho$, this surface term falls faster than $1/R_1$, therefore it does not give a contribution to the radiation potential. As is seen

from Eq. (10) Green's function has singularities at the points $\nu = m + 1/2$. In order to overcome this difficulty we assume a small imaginary part for n_0 and correspondingly for ν . As is noted in Ref. [13] the expression (10) is correct for complex values of ν . For these discrete values ν the integral (14) can be calculated analytically [16]. We present the results for $\nu = 1/2 + i\text{Im}[\nu_{1/2}]$ and $\nu = 3/2 + i\text{Im}[\nu_{3/2}]$, $\text{Im}[\nu] \ll 1$:

$$A_{1/2}(R) = -\frac{4e i \text{sgn}(\nu) K_0(k_0\rho)}{c \sinh(\pi \text{Im}[\nu_{1/2}])} \frac{\rho}{\sqrt{R^2 + \rho^2}},$$

$$A_{3/2}(R) = -\frac{8ie \text{sgn}(\nu)}{c \sinh(\pi \text{Im}[\nu_{3/2}])} \frac{\rho}{\sqrt{R^2 + \rho^2}}$$

$$\times [(k_0\rho)K_0(k_0\rho) - K_1(k_0\rho)], \quad R < R_1 \quad (15)$$

where $K_{0,1}$ are the modified Bessel functions of second kind [16] and a nonmagnetic medium ($\mu \equiv 1$) is assumed (see below). When obtaining Eq. (15) in the limit $R, R_1 \gg \rho$ we extend the integral limits in Eq. (14) to infinity and neglect all the terms smaller $1/R$. Note that the radiation potential depends only on the module of the vector \mathbf{R} . Nonisotropic terms are possible for nondiscrete values of ν ; however, they are small in terms of the parameter $1/R$. In order to find the radiation intensity, one should know the radiation fields in the vacuum region that matches the solutions given in Eq. (15).

In the absence of external sources, the isotropic solution of Eq. (6) is chosen in the form

$$A_\nu(R) = C \frac{e^{ikR}}{R}, \quad R > R_1. \quad (16)$$

The constant C should be found from the boundary conditions. Since there is not any current on the sphere R_1 ($\mathbf{R}_1 \neq \hat{\mathbf{z}}R_1$), the magnetic field is finite, and correspondingly we have (see, for example, Ref. [15])

$$\mathbf{n} \times \mathbf{A}_1 = \mathbf{n} \times \mathbf{A}_2, \quad (17)$$

where \mathbf{n} is unit vector normal to the boundary surface. In our case, this leads to the equation $A_\nu(R_1) = A_{1/2}(R_1)$. Using Eqs. (15) and (16) one finds

$$C_{1/2}(R_1) = -\frac{4ie \text{sgn}(\nu)}{c \sinh(\pi \text{Im}[\nu_{1/2}])} \rho K_0(k_0\rho) e^{-ikR_1}. \quad (18)$$

When obtaining Eq. (18) we assumed that $R_1 \gg \rho$. One can also find $C_{3/2}$ and other values of C for $\text{Re}[\nu] = m + 1/2$ in an analogous manner. For the nondiscrete values of ν , C can be found numerically (see Fig. 2). As follows from Fig. 2 one can expect any significant radiation emission only at frequencies for which $\nu = m + 1/2$.

IV. RADIATION INTENSITY

To find the radiation intensity, one should know the electric and magnetic fields far from the charge outside of the medium area $R > R_1 \gg \rho$ (see Fig. 1). Recall that the radiation vector potential is directed along the z axis and $\mathbf{A} \equiv A_z$. Therefore from Eq. (16) the magnetic field $\mathbf{B} = \nabla \times \mathbf{A}$ at the observation point R is given by the expressions

$$B_x(\mathbf{R}) = C \frac{ikR_y e^{ikR}}{R^2}, \quad B_y(\mathbf{R}) = -C \frac{ikR_x e^{ikR}}{R^2}, \quad B_z \equiv 0. \quad (19)$$

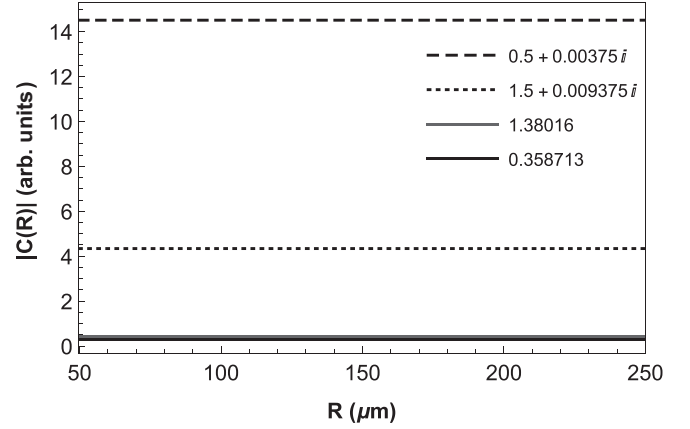


FIG. 2. $|C(R)|$ dependence on R for different values of ν when $n_0 = 5$, $\beta = 0.9$. Straight lines mean that $|A(R)| \sim 1/R$. The amplitude of the radiation is negligible for $\nu \neq m + 1/2$.

Here we keep only the terms which are proportional to $O(1/R)$ that give a contribution to the radiation intensity. The magnetic field energy density follows from Eq. (19):

$$U_B = \frac{|\mathbf{B}|^2}{8\pi} = |C|^2 \frac{k^2 \sin^2 \theta}{8\pi R^2}. \quad (20)$$

The electric field energy density in the vacuum is equal to the magnetic field energy density, and the radiation intensity is determined through the electromagnetic field energy density as $I(\theta) = cR^2 U$, where $U = 2U_B$. Using Eqs. (18) and (19) for the radiation intensity at $\text{Re}[\nu] = 1/2$, we have

$$I_{1/2}(\theta) = \frac{4e^2}{\pi c} \frac{k^2 \rho^2 K_0^2(k_0\rho)}{\sinh^2(\pi \text{Im}[\nu_{1/2}])} \sin^2 \theta. \quad (21)$$

It follows from Eq. (11) that for $n_0^2 = \varepsilon + i\text{Im}[\varepsilon]$, $\text{Im}[\varepsilon] \ll \varepsilon$, and $\nu = 1/2 + i\text{Im}[\nu_{1/2}]$:

$$k\rho = \frac{\sqrt{3}}{2\sqrt{\varepsilon}}, \quad \text{Im}[\nu_{1/2}] = \frac{3\text{Im}[\varepsilon]}{8\varepsilon}. \quad (22)$$

Substituting Eq. (22) into Eq. (21), we finally obtain

$$I_{1/2}(\theta) = \frac{3e^2}{\pi c} \frac{K_0^2\left(\frac{\sqrt{3}}{2\sqrt{\varepsilon}}\right)}{\sinh^2\left(\frac{3\pi \text{Im}[\varepsilon]}{8\varepsilon}\right)} \sin^2 \theta, \quad (23)$$

where $k = k_0\beta$ and $\beta = v/c$. Here we present a peak intensity corresponding to the wavelength $\lambda = 4\pi\sqrt{\varepsilon/3}\rho$ ($\text{Re}[\nu] = 1/2$). Similar expressions can be written for smaller peak intensities $\text{Re}[\nu] = 3/2$, etc. Intensities for nondiscrete frequencies are significantly smaller (see Fig. 1). It is well known [16] that the modified Bessel function K_0 is exponentially small for large values of the argument. Therefore from Eq. (23) we can state that for the existence of radiation, the following condition should be satisfied:

$$\beta > \frac{\sqrt{3}}{2\sqrt{\varepsilon}}. \quad (24)$$

This is the analog of Cherenkov condition [17] for the Maxwell's fish-eye profile. Note that the radiation considered here is the mix of Cherenkov and transition radiations; see also Ref. [10]. As follows from Eq. (24), the radiation emission

condition in the Maxwell’s fish-eye profile is weaker than the ordinary Cherenkov condition in the homogeneous medium with refraction index $\sqrt{\epsilon}$, $\beta > 1/\sqrt{\epsilon}$. However, it is stronger than the Cherenkov condition for the homogeneous medium with refraction index $2\sqrt{\epsilon}$. It is interesting that the condition obtained for totally inhomogeneous medium is very similar to the Cherenkov condition for the homogeneous medium.

As is seen from Eq. (23), the angular distribution of the intensity is like that of dipole radiation. Moreover, the maximum intensity is reached in the directions normal to the particle velocity.

Lossless medium: Nonisotropic radiation

The main difference is happening at the discrete frequencies $\nu = m + 1/2$. In this case, the radiation potential is determined through the generalized Green’s function (12). Our estimates show that the radiation potential at large distances $R \gg \rho$ behaves as

$$\tilde{A}_{1/2}(\mathbf{R}) \sim \frac{8e \operatorname{sgn}(\nu)}{\pi c} \int_{-R_1}^{R_1} dz \frac{(z^2 - \rho^2 - 4\rho^2 z \cos \theta/R)e^{ik_0 z}}{\sqrt{[(z - R \cos \theta)^2 + R^2 \sin^2 \theta](z^2 + \rho^2)[(z + \rho^2 \cos \theta/R)^2 + \rho^4 \sin^2 \theta/R^2]}} \arccos \frac{\rho^2 - z^2 - 4\rho^2 z \cos \theta/R}{z^2 + \rho^2}. \tag{26}$$

Unfortunately this integral cannot be taken analytically, and we are forced to use some numerical estimations. Nevertheless we will try to collate analytic and numerical results and make qualitative predictions of radiation properties in different cases. The second term in Eq. (12) for $\operatorname{Re}[\nu] = 1/2$ has an isotropic character and is analogous to the regular case in Eq. (10). It is obvious that at small angles $\theta \rightarrow 0$, the main contribution to the integral (26) gives the pole at $z = -\rho^2 \cos \theta/R$. Conversely, the contribution of the pole $z = R \cos \theta$ at large distances is negligible because of the oscillations $e^{ik_0 z}$ in the integral. We present the results of numerical estimates of the integral Eq. (26) in Figs. 3 and 4. As follows from Fig. 3 at large distances the potential behaves as $\sim 1/R$. However, the amplitude is different for different observation angles, contrary to the case in the previous paragraph.

Finally we present the radiation intensity for the impedance match medium $\mu(r) = \epsilon(r) = n(r)$ (see Ref. [4]):

$$I_{1/2}^i(\theta) = \frac{9e^2}{\pi c} \frac{K_1^2\left(\frac{\sqrt{3}}{2\beta\sqrt{\epsilon}}\right)}{\epsilon\beta^2 \sinh^2\left(\frac{3\pi \operatorname{Im}[\epsilon]}{8\epsilon}\right)} \sin^2 \theta. \tag{25}$$

Comparing with the nonmagnetic medium case Eq. (23) one can see that the main difference is the additional particle energy dependence ($\sim 1/\beta^2$).

The radiation potential in the lossless medium is highly anisotropic. It follows from Fig. 3 that at large observation angles the potential is significantly smaller. The maximum potential is reached at small angles from the particle trajectory. Modifying the imaginary part of n_0 , one can observe a transition from highly directed to isotropic radiation potential. As is shown above, the isotropic radiation potential leads to a dipole-like radiation intensity. However, in the lossless medium the radiation potential is highly directed. Note that the R dependence for all angles is $\sim 1/R$; see Fig. 3. The straight lines in Fig. 3 represent the radiation potentials for different values of $\operatorname{Im}[n_0]$ calculated via Eq. (15). The U -shaped curve is obtained for the lossless medium using generalized Green’s function (12) and (26). The actual radiation potential is determined by the curve below the straight lines.

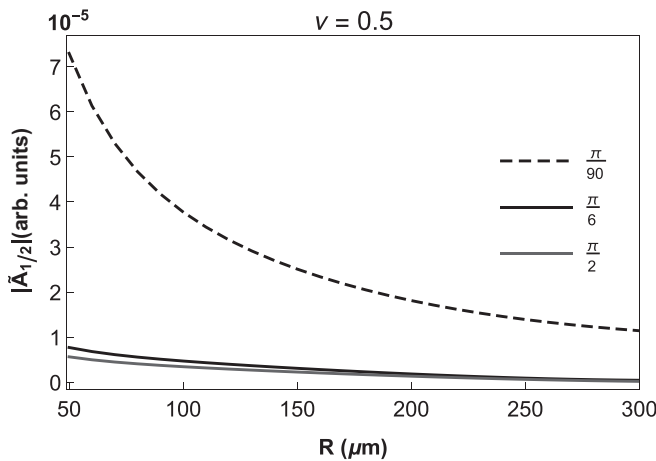


FIG. 3. R dependence of radiation potential given by Eq. (26) for different angles. Here we take the observation point on the cutting boundary $R \equiv R_1$.

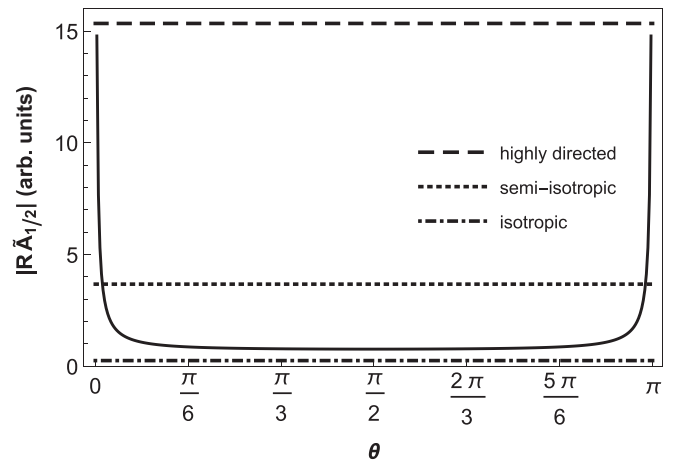


FIG. 4. Angular distribution of radiation vector potential. Straight lines are the potentials for the media with losses for different values of refraction index imaginary part.

Therefore one can distinguish three different regimes of radiation depending on the losses of the medium ($\text{Im}[n_0]$); see Fig. 4.

Physically, the above-mentioned transition from one angular distribution to another can be understood in the following way. The vector potential of a moving charge in the vacuum behaves like $A_0(R) \sim K_0(\sqrt{k_0^2 - k^2 R} |\sin \theta|)$. This means that it is concentrated around the direction of the particle's velocity because for large arguments K_0 falls exponentially. This alone is not a photonic field yet. When one adds a nonhomogeneous medium these pseudophotons scatter, becoming real photons. In the Maxwell's fish-eye medium without losses, photons are totally reflected from layers with a decreasing refraction index. Because of the total internal reflection, those remain around the charge. When the losses are taken into account, photons evanescently penetrate through the layers and eventually result in the isotropic angular distribution for large enough losses, as seen in Fig. 3. This transition is similar to the phenomenon of attenuated total reflection; see, for example, Ref. [18].

V. CONCLUSION AND DISCUSSION

We have considered the radiation from a charged particle moving through a medium with Maxwell's fish-eye refraction index profile. The spectrum of radiation has a discrete character. The main emitted wavelength is proportional to the radius of refraction profile $\lambda = 4\pi\sqrt{\epsilon/3}\rho$. In the regular medium (with losses) the radiation has a dipole character, whereas in the lossless medium it is highly directed. In the intermediate regime with moderate losses radiation will be nonisotropic.

So far we assumed that the particle trajectory along z passes through the origin. If the trajectory is at some distance d from the origin, then the corresponding current density is determined as

$$\mathbf{j}(\mathbf{r}, \omega) = e \frac{\mathbf{v}}{v} \delta(x - d_x) \delta(y - d_y) e^{ik_0 z}. \quad (27)$$

Similar calculations show that all expressions keep their form except ρ in the argument of the Bessel function (21), where one should substitute it with $\sqrt{\rho^2 + d^2}$ where $d^2 = d_x^2 + d_y^2$. So for the main emitted wavelength $\lambda = 4\pi\sqrt{\epsilon/3}\rho$, one has

$$I_{1/2}^d(\theta) = \frac{3e^2 K_0^2 \left(\sqrt{\frac{3}{4\epsilon} + k^2 d^2} \right)}{\pi c \sinh^2 \left(\frac{3\pi \text{Im}[\epsilon]}{8\epsilon} \right)} \sin^2 \theta. \quad (28)$$

Correspondingly, the Cherenkov condition acquires the form

$$\beta > \frac{\sqrt{3}}{2\sqrt{\epsilon}} \sqrt{1 + \frac{d^2}{\rho^2}}. \quad (29)$$

This condition means that the impact distance should be smaller than the emitted wavelength $d < \lambda/2\pi$.

In the anisotropic case the radiation potential depends on not only the ratio d/λ as in the isotropic case but also d/ρ . Therefore here the restriction on the impact parameter is stronger, $d/\rho \ll 1$.

Note that Maxwell's fish-eye millimeter scale systems already exist in two dimensions [19] as well as in three [20]. Therefore they can be used for the generation of radiation in microwave and terahertz regions. As is seen from Eq. (19), radiation intensity does not depend on the cutting parameter R_1 (except in the lossless medium case). This means that real systems with the Maxwell's fish-eye profile can have a size of order radius ρ [19,20].

ACKNOWLEDGMENTS

The authors are grateful to Armen Allahverdyan and Arsen Hakhoumian for useful discussions and comments. This work was performed with partial financial support from the Armenian Committee of Science, Grant No. 18T-1C082 (Z.G.).

-
- [1] M. Born and E. Wolf, *Principles of Optics*, 4th ed. (Pergamon Press, Oxford, 1970).
- [2] U. Leonhardt, *Science* **312**, 1777 (2006); *New J. Phys.* **8**, 118 (2006).
- [3] U. Leonhardt, *New J. Phys.* **11**, 093040 (2009).
- [4] U. Leonhardt and T. G. Philbin, *Phys. Rev. A* **81**, 011804(R) (2010).
- [5] R. J. Blaikie, *New J. Phys.* **12**, 058001 (2010).
- [6] L. A. Pazynin, V. L. Pazynin, and H. O. Sliusarenko, *IEEE Trans. Antennas Prop.* **63**, 4393 (2015).
- [7] J. Perczel, P. Kómár, and M. D. Lukin, *Phys. Rev. A* **98**, 033803 (2018).
- [8] K. Dadashi, H. Kurt, K. Ustun, and R. Esen, *J. Opt. Soc. Am. B* **31**, 2239 (2014).
- [9] Zh. Gevorgian, M. Davtyan, and A. Nersisyan, *Phys. Rev. A* **101**, 023840 (2020).
- [10] Y. Liu and L. K. Ang, *Sci. Rep.* **3**, 3065 (2013).
- [11] C.-T. Tai, Differential operators in vector analysis and the Laplacian of a vector in the curvilinear orthogonal system, Tech. Rep., Radiation Laboratory, University of Michigan, Ann Arbor (1990); C.-T. Tai, *Dyadic Green Functions in Electromagnetic Theory*, 2nd ed. IEEE Press Series on Electromagnetic Waves (IEEE Press, 1993).
- [12] Yu. N. Demkov and V. N. Ostrovskii, *Zh. Eksp. Teor. Fiz.* **60**, 2011 (1971) [*Sov. Phys. JETP* **33**, 1083 (1971)].
- [13] R. Szmytkowski, *J. Phys. A: Math. Theor.* **44**, 065203 (2011).
- [14] L. A. Pazynin and G. O. Kryvchikova, *Prog. Electromagnetics Res.* **131**, 425 (2012).
- [15] W. C. Chew, [arXiv:1406.4780v1](https://arxiv.org/abs/1406.4780v1).
- [16] I. S. Gradshteyn and I. M. Ryzhik, *Table of Integrals, Series, and Products*, 7th ed. (Academic Press, Burlington, MA, 2007).
- [17] M. L. Ter-Mikaelian, *High-Energy Electromagnetic Processes in Condensed Media* (John Wiley and Sons, New York, 1972).
- [18] P. Larkin, *Infrared and Raman Spectroscopy*, 1st ed. (Elsevier, Waltham, MA, 2011).
- [19] D. Headland, M. Fujita, and T. Magatsuma, *Opt. Express* **28**, 2366 (2020).
- [20] H. F. Ma, B. G. Cai, T. X. Zhang, Y. Yang, W. X. Jiang, and T. J. Cui, *IEEE Tran. Antennas Prop.* **61**, 2561 (2013).